Pergamon

Deep-Sea Research I, Vol. 41, No. 4, pp. 721–739, 1994

0967–0637/94 $7.00 + 0.00

INSTRUMENTS AND METHODS

In situ measurement of fluid flow from cold seeps at active continental margins

P. LINKE,* E. SUESS,* M. TORRES,* V. MARTENS,† W. D. RUGH,‡ W. ZIEBIS* and L. D. KULM‡

(*Received* 27 *May* 1992; *in revised form* 27 *October* 1992; *accepted* 2 *December* 1992)

Abstract—*In situ* measurement of fluid flow rates from active margins is an important parameter in evaluating dissolved mass fluxes and global geochemical balances as well as tectonic dewatering during developments of accretionary prisms. We have constructed and deployed various devices that allow for the direct measurement of this parameter. An open bottom barrel with an exhaust port at the top and equipped with a mechanical flowmeter was initially used to measure flow rates in the Cascadia accretionary margin during an *Alvin* dive program in 1988. Sequentially activated water bottles inside the barrel sampled the increase of venting methane in the enclosed body of water. Subsequently, a thermistor flowmeter was developed to measure flow velocities from cold seeps. It can be used to measure velocities between 0.01 and 50 cm s^{-1}, with a response time of 200 ms. It was deployed again by the submersible *Alvin* in visits to the Cascadia margin seeps (1990) and in conjunction with sequentially activated water bottles inside the barrel. We report the values for the flow rates based on the thermistor flowmeter and estimated from methane flux calculations. These results are then compared with the first measurement at Cascadia margin employing the mechanical flowmeter. The similarity between water flow and methane expulsion rates over more than one order of magnitude at these sites suggests that the mass fluxes obtained by our *in situ* devices may be reasonably realistic values for accretionary margins. These values also indicate an enormous variability in the rates of fluid expulsion within the same accretionary prism.

Finally, during a cruise to the active margin off Peru, another version of the same instrument was deployed via a TV-controlled frame within an acoustic transponder net from a surface ship, the R.V. *Sonne*. The venting rates obtained with the thermistor flowmeter used in this configuration yielded a value of 441 l m^{-2} day^{-1} at an active seep on the Peru slope. The ability for deployment of deep-sea instruments capable of measuring fluid flow rates and dissolved mass fluxes from conventional research vessels will allow easier access to these seep sites and a more widespread collection of the data needed to evaluate geochemical processes resulting from venting at cold seeps on a global basis. Comparison of the *in situ* flow rates with rates from steady-state compactive dewatering models differ by more than 4 orders of magnitude. This implies that only a small area of the margin is venting and that there must be recharge zones associated with venting at convergent margins.

*GEOMAR Research Center for Marine Geosciences, D-24148 Kiel, Germany.
†Institut für Meereskunde, D-24105 Kiel, Germany.
‡College of Oceanography, Oregon State University, Corvallis, OR 97331-5503, U.S.A.

INTRODUCTION

FLUID venting at subduction zones is a current research frontier (SUESS *et al.*, 1985; KULM *et al.*, 1986; MOORE, MASCLE *et al.*, 1987; BOULÈGUE *et al.*, 1987; CARSON *et al.*, 1990; CARSON and HOLMES, 1991; MOORE, 1991; MOORE *et al.*, 1991). Rates of water discharge and dissolved material flux rates are parameters of the highest significance to marine scientists, but only a few attempts of direct measurements exist (CARSON *et al.*, 1990; SAYLES and DICKINSON, 1991 and references cited therein). Very high temperatures coupled with jet-like discharge velocities of fluids at mid-ocean ridge systems require special corrosion-resistant materials for these vents to become accessible to direct experiments. Fluid venting at plate subduction zones, on the other hand, result in small temperature anomalies at the sediment–water interface (cold seeps) and the water is expelled at imperceptibly slow rates.

We have developed a concept for determining water and dissolved material flux rates at subduction zones, and have designed a simple instrument to isolate, collect and measure the flow rates of vent fluids. In designing this equipment we made use in the beginning of existing and proven technologies that could be assembled with off-the-shelf components. This initial instrument, which we termed the "Benthic Barrel", was successfully deployed several times by the D.S.R.V. *Alvin* in 1987, 1988 and 1990 at vent sites of the Cascadia subduction zone and some of the initial measurements from these deployments have already been published (CARSON *et al.*, 1990). In this paper we document the initial design of the OSU Benthic Barrel, which has not been published in detail, subsequent improvements involving a more sophisticated flowmeter, and present additional data sets of methane flux and water flow rates for the Cascadia accretionary margin (675 and 2424 m water depth, Table 1). These results show the applicability of using short-term experiments from submersibles to obtain such data. Furthermore, we report the recent development of a TV-controlled device (VEnt SPider—VESP) for deployment of a new (GEOMAR) Benthic Barrel from a conventional surface research vessel, eliminating the need and associated costs of deployment by submersible. This device was sucessfully deployed on a seep site at the Peru margin from board the R.V. *Sonne*. The results obtained are compared with those from a background station in the abyssal plain of the northern Peru Basin. These direct measurements of fluid flow rates are then discussed in the context of estimates obtained using hydrologic models (BEKINS and DREISS, 1992) and subbottom temperature measurements (DAVIS *et al.*, 1990; LE PICHON *et al.*, 1992; HENRY *et al.*, 1992) from the Cascadia and the Nankai accretionary margin.

CONCEPT

The Benthic Barrel is a cylindrical chamber with a large opening at the bottom and a small exhaust port at the top. The chamber is deployed over a suspected vent site with the purpose of channelling the effluent from the sea floor into a semi-enclosed environment. The internal volume of the chamber is initially flooded with ambient seawater and is then slowly replaced by vented fluids. In this way a water mixture develops within the chamber with increasing amounts of vent fluid. Sequentially timed water samples are collected during deployment by bottles mounted inside the chamber. Changes in the concentration of dissolved components among these bottles are then used to calculate their flux rates (CARSON *et al.*, 1990).

The exhaust port at the top of the chamber accepts either a mechanical flowmeter or a hot-bead-thermistor flowmeter, both calibrated for a wide range of flows. The mechanical flowmeter is inserted by the manipulator arm of a submersible into the exhaust port upon completion of the internal water sampling cycle. The thermistor flowmeter can be permanently mounted at the Benthic Barrel, and it directly records the flow rate from the chamber. The reading of the mechanical meter is monitored photographically from the submersible, whereas the signal of the thermistor flowmeter is continuously recorded and stored via cable on board the submersible during the entire sampling period. Temperature changes are also monitored during the deployment period by a temperature sensor mounted inside the chamber.

Since the costs of deep-sea submersibles are rather high, we developed a TV-controlled device for deployment of the Benthic Barrel from a conventional surface research vessel. The barrel is attached to the central piston of a modified multicorer frame (Barnett *et al.*, 1984), which operates on a water hydraulic basis and assures gentle deployment of the barrel once the frame settles on the sea floor. The GEOMAR Barrel is equipped with five water bottles and a storage CTD probe, which is used to activate the water-sampling cycle and to continuously record conductivity, temperature, pressure and flow data.

INSTRUMENTATION

OSU Barrel

A commercially available 55-gallon polyethylene barrel constitutes the shell of the benthic chamber (Fig. 1). It is fitted with a removable lid, an O-ring seal and a bolt-on retaining ring. The internal instrumentation is attached to the lid and can be easily removed from the shell as a unit, giving access to the water bottles and timer for sampling and staging. A 3.3-cm diameter hole—the exhaust port—is centered on two polycarbonate plate rings in the lid. This opening allows fluid to escape and serves as a port for inserting the flowmeter. The barrel is open at the bottom so that it can be pushed into the sediment a short distance, thereby forming a seal over the seep site. A flared skirt about 25 cm wide, made of three overlapping sections of silicon rubber, can be fitted around the bottom edge of the barrel to ensure a seal at sites where poor sediment penetration is expected. An anchor chain or other weights may be wrapped around the outside of the barrel (about 20 cm above the bottom edge) to facilitate penetration and to add vertical stability (Plate 1D). Two stainless steel bands (not shown in Fig. 1 but visible in Plate 1D), mounted to the outside of the barrel with polypropylene line, provide a harness for deploying, positioning, and recovering the instrument via submersible. The barrel encloses 0.26 m^2 of the bottom surface area and has an internal displaceable volume of 180 l.

Six General Oceanics 2-l Niskin™ bottles are mounted vertically around a cylindrical polycarbonate frame. The bottles are tripped sequentially by a motor-driven plate with a wedge mounted off-center (Fig. 1). As the plate turns, the wedge consecutively depresses the tripping piston of each Niskin™ bottle. The motor, controller-electronics and batteries are contained in an aluminum pressure case mounted in the center of the polycarbonate frame. The controller, a model IV "Tattletale" Micro-computer (Onset Computer Corporation), provides motor control and position sensing, analog to digital conversion and internal battery level monitoring. It is powered by a single 9-V battery. Sample collection times are pre-programmed to the desired day/hour/minute before the

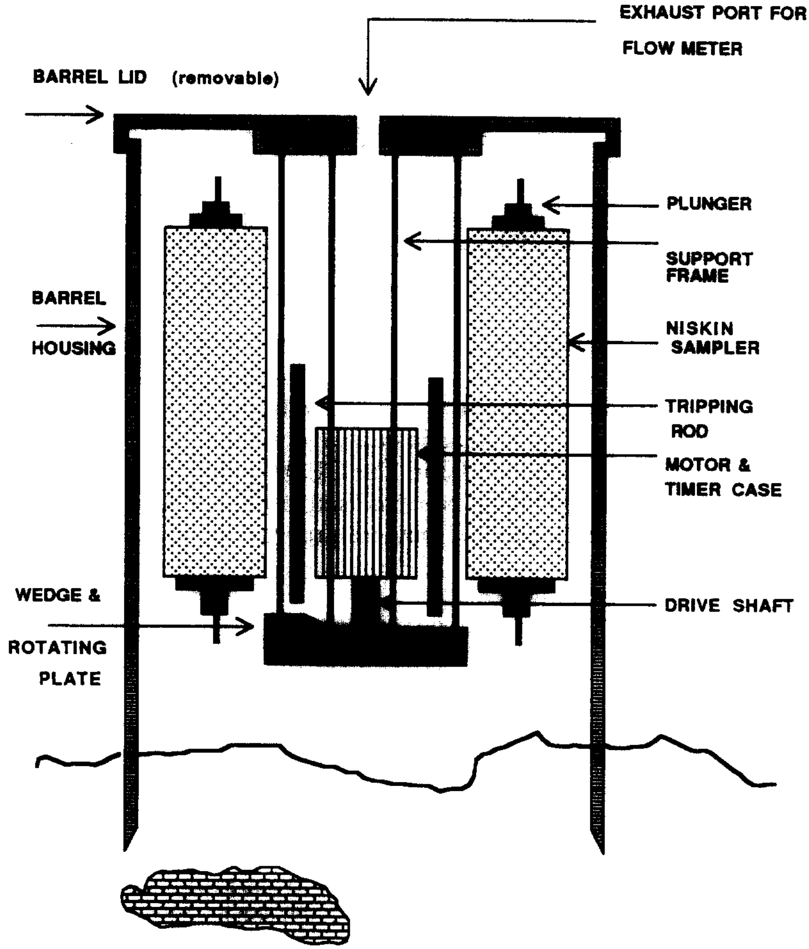

Fig. 1. Schematic diagram of the Benthic Barrel and its components shown deployed on the sediment with a subsurface carbonate concretion.

dive. The high-torque DC gear motor is powered by four standard 9-V batteries. The motor shaft coupled to a drive shaft penetrates the pressure case through a double O-ring seal. The shaft also drives a concentric cylinder in which six narrow slots are cut; these slots pass between an infra-red emitter-detector pair to give positional signals. Temperature readings (to an accuracy of 0.01°C) are taken before each sample is collected and the data are stored in the controller. In contrast to the much smaller device of SAYLES and DICKINSON (1991), the OSU Barrel does not contain a stirring device for mixing of the internal volume; this was not deemed necessary due to the stirring effect that results from the closing of the bottles inside the barrel housing by means of the two large plungers on each end.

Flowmeters

The mechanical and thermistor flowmeters are mounted in interchangeable assemblies (Fig. 2), which are inserted into the opening at the top of the barrel (Plate 1D,E). Each

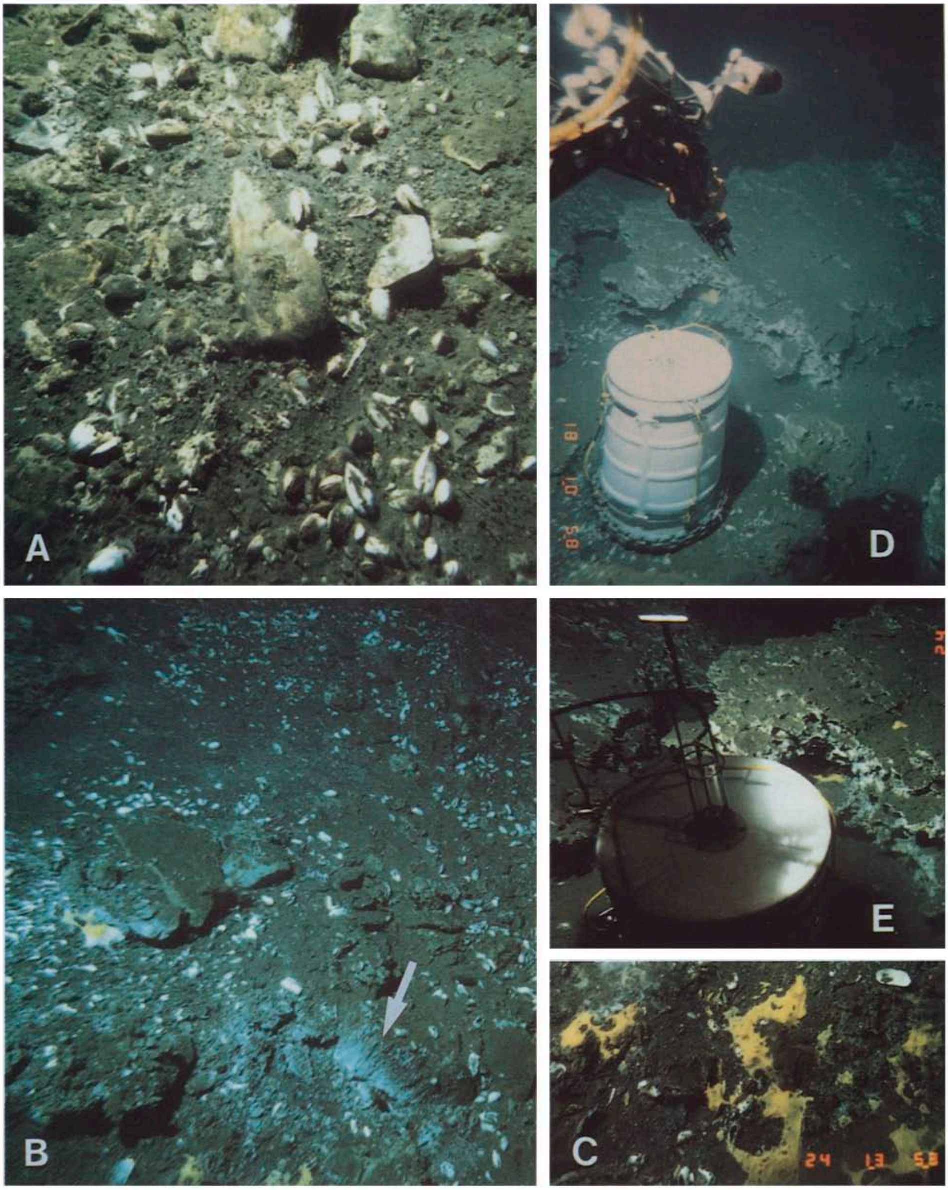

Plate 1. (A) Active seep site with clam colonies consisting of live and dead *Calyptogena* sp. in clusters around cold seep. Size of clams: 10–15 cm. (B) White streaks on the rock surface (arrow) reveal an active seep surrounded by *Calyptogena* sp. clams and bacterial mats (C). (D) OSU Barrel deployed at Cascadia seep site (*Alvin* dive 2283); the barrel is 92 cm high, the exhaust port atop the barrel is open (without flowmeter inserted) and a heavy chain aids in forming a seal at the sediment surface. During the deployment of the OSU Barrel at the active gas hydrate site on the Cascadia margin a vigorous methane flux was measured from the sequential water samples taken within the barrel. (E). OSU Barrel with inserted thermistor flowmeter.

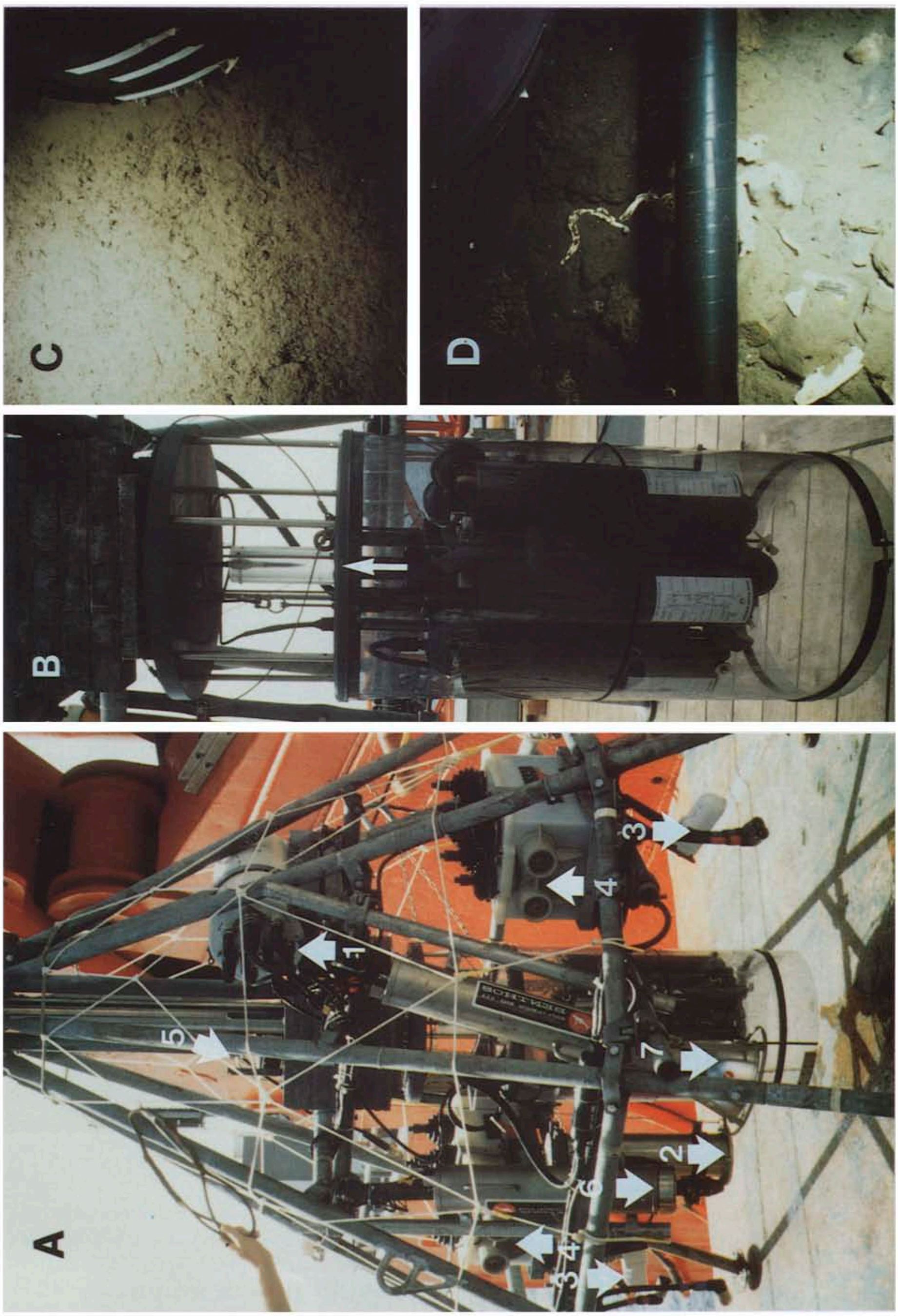

Plate 2.

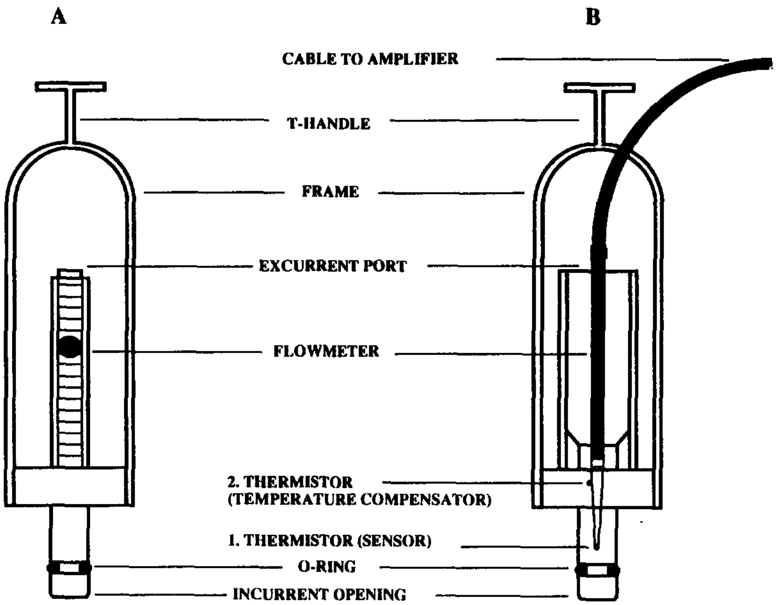

Fig. 2. (A) Mechanical (Bernoulli-type) and (B) thermistor flowmeter mounted inside a stainless steel cage with T-bar handle for submersible operation; the opening with the O-ring seal fits the exhaust port of the barrel; radius of the pipe: 1.3 cm.

assembly consists of a flowmeter mounted inside a PVC pipe (2.6-cm inner diameter) and a stainless steel cage with a T-bar handle for manipulation by the submersible. The end of the PVC-pipe is fitted with a silicon rubber O-ring (Fig. 2) to provide a seal between the flowmeter and the polycarbonate ring in the barrel lid.

The mechanical meters, three Gilmont™ precision flowmeters were calibrated for separate but overlapping ranges from 0.01 to 4.0 ml min^{-1}, so that a wide range of fluid flow rates could be measured *in situ*. Calibration of this flowmeter is an elaborate procedure described elsewhere (Carson *et al.*, 1990); it includes fluid viscosity as a

Plate 2. (A) VESP (VEnt SPider) on the deck of the R.V. *Sonne*. The main frame, a modified multicorer, carries: (1) an underwater video-telemetry system; (2) a low-light TV-camera; (3) two flood lights; (4) two batteries; (5) a transponder used as subtransponder; (6) a camera; and (7) a flash for a TV-controlled deployment, exact positioning, and documentation of the deployment site. (B) View of the GEOMAR Barrel with the transparent shell (inner diameter 41.4 cm) on the deck of the R.V. *Sonne*. The internal instrumentation is attached to the central piston of the multicorer; the shell can be easily removed. Five 2-l water bottles and a storage CTD are mounted vertically around a cylindrical stainless steel frame; the bottles are tripped sequentially by a motor in the center of this frame. The central exhaust port (arrow) allows fluids to escape, which are channelled through a pipe to the centrally mounted thermistor flowmeter. (C) TV-guided deployment of the GEOMAR Barrel from the R.V. *Sonne* at Sta. 152-17 in the northern Peru Basin. This deployment is regarded as a background station without active venting to obtain an *in situ* flow baseline (see Fig. 6). Note the good seal between the soft sediment surface and the transparent barrel shell. (D) TV-guided deployment of the GEOMAR Barrel from the R.V. *Sonne* at Sta. 168-2, an active seep site at the Peru margin. The sediment surface at this site was rough and covered with mudstones and clam shells, but with only a thin layer of sediment, allowing only little penetration of the polyethylene barrel shell.

function of temperature, pressure and salinity as well as material compressibilities. The calibration also compensates for the reduction of flow induced by back-pressure when the natural flow of vent water from the sampling area (0.26 m^2) is channelled through the small orifice of the flowmeter (approx. 3 mm^2). The correction factor for calculating the "true" flow from the "metered" flow is non-linear and depends on the total magnitude of flow.

The thermistor (hot-bead) flowmeter (modified after LaBarbera and Vogel, 1976) can be used to measure flow velocities from about 0.01 to 50 cm s^{-1}, with a response time of about 200 ms and a spatial resolution of about 1 mm. The circuit has low power requirements due to a self-balancing bridge circuit that minimizes the requisite thermistor heating. Data are encoded in terms of frequency and continuously recorded on a casette tape recorder. The flowmeter is centered in the pipe mounted on the exhaust port of the barrel and consists of a stainless steel rod with a plastic Eppendorf™ pipette tip. The tip is filled with epoxy resin, embedding the two bead thermistors (Fig. 2B). The bead at the top of the tip is used as the sensing thermistor (Fenwal Electronics, GD22J1, 200 Ω/25°C, stub end glass coated, 0.9 mm in diameter), whereas a glass encapsulated bead (Fenwal Electronics, GB35J1, 5 KΩ/25°C) serves as the temperature compensator.

In this design, the potential difference across the bridge circuit is approximately proportional to the logarithm of the flow velocity. The nonlinear scale can be a disadvantage in some applications, but it does allow high sensitivities to low-speed flows without interruption due to momentary exposures to higher speeds (such as passing waves). The flowmeter is connected to the submersible by a 9 m long cable that allows the data to be recorded inside the submersible. The potential across the bridge circuit is amplified and the voltage needed to heat the sensing thermistor in stagnant (zero flow) water is subtracted. The amplifier contains a voltage-to-frequency converter with a (low power) timer (Texas Instruments ICM7555) used as an astable multivibrator. The pulse repetition rate varies from about 300 to 1500 Hz and is recorded on an inexpensive battery-powered tape recorder. A rechargeable power pack (24–30 V, current drain 100–200 mA) provides the possibility of having a fully portable and power independent board unit. To recover the data from the magnetic tape a frequency-to-voltage converter is used.

Calibration of the thermistor flowmeter unit

The flowmeter was temperature-compensated in two water baths with stagnant (zero flow) water (after LaBarbera and Vogel, 1976) at −1 and +4°C. The calibration was conducted in an arrangement similar to that described by Vogel (1981), where water emerges from a long pipe (1.2 m length; 0.98 cm radius) at rates determined with the aid of an overflow and a graduated cylinder. Both procedures were carried out in a temperature-controlled room at +1°C. The signals of the flowmeter, which is positioned at the end of the pipe, are visible on the 0–50 μA meter of the amplifier and are recorded on a strip chart recorder and encoded on tape. Assuming laminar flow, the mean velocity (U) can be calculated by dividing the water flow (F = volume per time) by the area (A) of the pipe:

$$U\ (\text{cm s}^{-1}) = F\ (\text{cm}^3\ \text{s}^{-1})/A\ (\text{cm}^2). \qquad (1)$$

As shown in Fig. 3A the output of the flowmeter approximates a logarithmic function, indicating a higher sensitivity of the flowmeter for smaller velocities. On a semi-logarithmic plot (Fig. 3B) the conversion of the flowmeter signal on the strip cart recorder

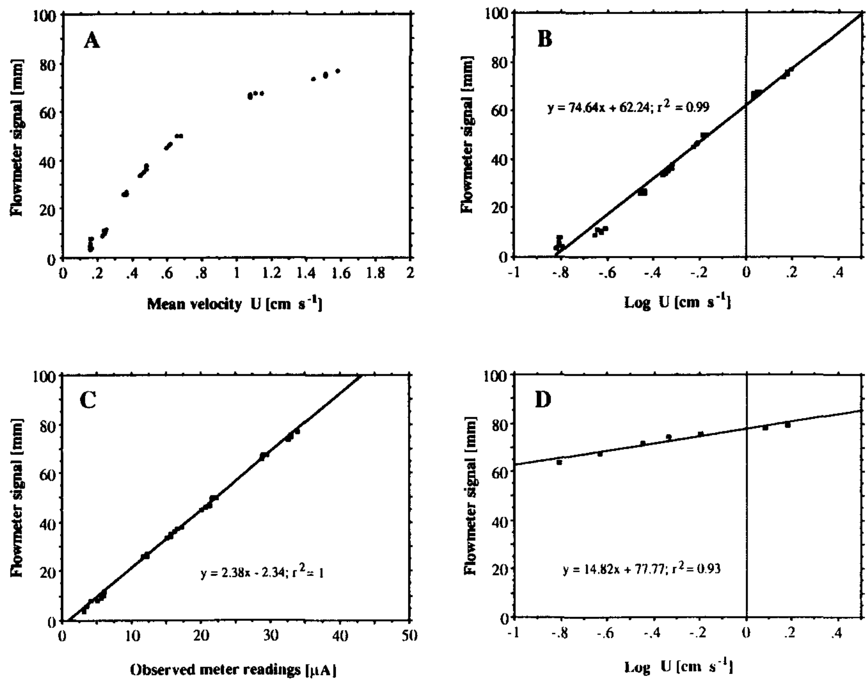

Fig. 3. (A) Thermistor flowmeter calibration plot, mean velocity (U) versus flowmeter signal on a strip chart recorder, demonstrating that the output of the flowmeter approximates a logarithmic function. (B) Semi-logarithmic thermistor flowmeter calibration plot, log U versus flowmeter signal on a strip chart recorder. The regression of the calibration graph is used for the conversion of the flowmeter signal to velocity. (C) Linear calibration plot with flowmeter signals observed as meter readings versus recorded signals on a strip chart recorder. (D) Semi-logarithmic thermistor flowmeter calibration graph, log U versus flowmeter signal after recovery from the magnetic tape on a strip chart recorder.

(mm) to velocity corresponds to the regression of the calibration graph which is described by the function:

$$\text{Flowmeter signal (mm)} = a \times \log U + b \tag{2}$$

$$U\ (\text{cm s}^{-1}) = 10^{((\text{mm})-b)/a}. \tag{3}$$

Therefore, by using the regression of the calibration graph (Flowmeter signal (mm) = 74.64 × log U + 62.24; r^2 = 0.99; in Fig. 3B) the flowmeter signal can be converted to velocity:

$$U\ (\text{cm s}^{-1}) = 10^{((\text{mm})-62.24)/74.64}. \tag{4}$$

The linear correlation (Fig. 3C) between flowmeter signal (mm) on the strip chart recorder and the observed meter readings (μA) is described by the function:

$$\text{Flowmeter signal (mm)} = 2.38 \times (\mu\text{A}) - 2.34; \quad r^2 = 1. \tag{5}$$

The encoded (recorded on tape) flowmeter signals are decoded (played back from tape) on the strip chart recorder and converted to velocity according to the regression shown in Fig. 3D (decoded signal (mm) = 14.82 × log U + 77.77; $r^2 = 0.93$):

$$U\ (\mathrm{cm\ s^{-1}}) = 10^{((\mathrm{mm}) - 77.77)/14.82}. \qquad (6)$$

VESP (VEnt SPider) and GEOMAR Barrel

For TV-guided remote deployment from a conventional surface research vessel the barrel is lowered to the sea floor using the main frame of a modified multicorer (BARNETT *et al.*, 1984, see Plate 2A). The frame is constructed from steel pipes connected by scaffolding clamps; it has a total height of 3.5 m and a base that covers 7 m^2. The addition of further diagonal pipes provides more stability, and a platform for mounting of accessory equipment. The frame carries an underwater video-telemetry system (Preussag Meerestechnik 1987) consisting of a telemetry unit (Preussag, GC 1-87/U1), a low light TV-camera (Osprey, OE 0111-6006), two flood lights (ROS, 24V, 150 W halogen) and two batteries (Ocean Power, each 12 V, 230 A). The underwater telemetry unit communicates with that aboard ship (Preussag, GC 1-87/B1) and controls the various functions such as data and video transfer, power supply and triggers the sampling cycle of the barrel. The cable harness is attached to the frame (Burton underwater plugs). The frame also carries a transponder (EG&G, 723A used as subtransponder, 11 kHz receive-interrogate, 9 kHz reply-transmit) for exact positioning of the instrument within a transponder field; as well as a camera (Benthos, Edgerton standard camera, 372) and flash (Benthos, standard flash, 382) for documentation of the deployment site.

The GEOMAR Barrel is attached to the central piston of the above described multicorer frame, which operates on a water hydraulic basis and assures gentle deployment of the barrel on the sediment surface once the frame has reached the sea floor (Plate 2B). The depth of penetration depends on the softness of the sediment and can be adjusted by a stopper clamp to the height of the barrel. The outer shell of the barrel is exchangeable: during deployment from a submersible as was the case with the D.S.R.V. *Nautile* (DIA *et al.*, submitted) a transparent PVC-shell is advantageous, whereas for deployment from a surface vessel a more rigid polyethylene shell is required. For deployment during the R.V. *Sonne* cruise in 1992 we used a commercially available 55-gallon polyethylene barrel as the shell of the benthic chamber. The bottom of the barrel is cut away as with the OSU Barrel so that it can be pushed into the sediment forming a seal over the vent site. It encloses 0.238 m^2 of the sediment surface and has an internal displacement volume of 284 l. The transparent PVC shell used alternately covers 0.135 m^2 of the sediment surface and has an internal displacement volume of 100 l.

A 6 cm diameter hole—the exhaust port—is centered in the lid to allow fluids to escape and to serve as a port for mounting the thermistor flowmeter. The flowmeter is centrally mounted near the top end of a thick-walled tube, which at its lower internal circumference is funnel-shaped to channel the outflowing fluids from the barrel into the pipe (33.5 mm inner diameter; 8.81 cm^2 orifice). The thermistor flowmeter was calibrated (using the procedure described above) at 1.7°C, close to the *in situ* temperature at the deployment sites.

The internal instrumentation is attached to a central stand, and the shell can be easily removed from it to provide access to the water bottles and the storage CTD probe for sampling, programming and data recovery. Five 2-l water bottles (Hydrobios) are mounted vertically around a cylindrical stainless steel frame; the bottles are tripped sequentially by a motor in the center of this frame just as with the OSU Barrel. The sampling cycle is activated either by a reed contact switch, pulled by the mechanical arm from a submersible or by the buoyancy of a small piece of syntactic foam or, in case of deployment from a surface vessel, by the telemetry unit on board ship.

A storage CTD probe (ADM Elektronik GmbH) is also mounted on the frame. Both the motor and the storage CTD probe are contained in a titanium pressure case (Hydrobios, 6000 dBar). The electronic components are mounted on a main logic board and consist of an AC/DC converter, RS 232 transmitter/receiver, microprocessor (32 kB EPROM), storage unit (4 kB and 124 kB RAM), quartz clock and six bridge circuits. The storage CTD probe can be connected to a portable hand terminal (ADM, Termi 120), which serves as a control, display and storage unit. With this device the water sample sequence (the trigger interval, which can be set between 1 and 120 min), the calibration coefficients, the setting and installation of the sensors (time or pressure dependent), the duration of one measuring cycle (0.5–32 cycles s^{-1} or min^{-1}) and the averaging of scanned data are programmed before deployment. Thereby the storage probe can be optimally adjusted for the duration of a deployment.

Deployment procedure

The VESP is lowered from the surface vessel by the ship's (R.V. *Sonne*) coaxial cable (18.2 mm diameter, 7100 m length, 50Ω). Thirty meters above the instrument two syntactic foam floats (Euroshore, FM 280, each 27.9 kp buoyancy) are attached to the cable to keep it away from the instrument during deployment. VESP is lowered to 2–5 m above the sea floor and a place for deployment is selected by observing the TV-monitor while the ship proceeds at a speed of about 1 kn. The position of VESP is tracked within the transponder net for exact positioning or to repeatedly visit an attractive location (e.g. an active vent site as indicated by clusters of living *Calyptogena* clams). If the vent site is considered active, the VESP is then lowered immediately (within a few seconds) to the sediment surface and approximately 20 m of slack cable are released. Depending on weather, current velocities, positioning capabilities and navigatory skills of ship and crew, further slack has to be given to avoid disturbance during the sampling procedure. When the frame achieves bottom contact, the central piston with the attached barrel is slowly drawn down by its own weight towards the sediment surface. The penetration and sealing of the barrel is observed on the TV-monitor, as well as any movements of the frame due to insufficient slack of the ship's cable. After waiting for the resuspensed particles to settle or being swept away, the water sampling sequence and the data recording are activated by the trigger from the on-board telemetry unit.

RESULTS

Submersible-guided deployments

During *Alvin* Dive 2283 the OSU Barrel was placed for approximately 3 h over a densely populated colony of *Calyptogena* clams and bacterial mats (Plate 1A–C), a benthic community known to thrive at active vent sites (SUESS *et al.*, 1985). A zero flow signal of 7 μA was observed and recorded while the thermistor flowmeter remained in a bucket

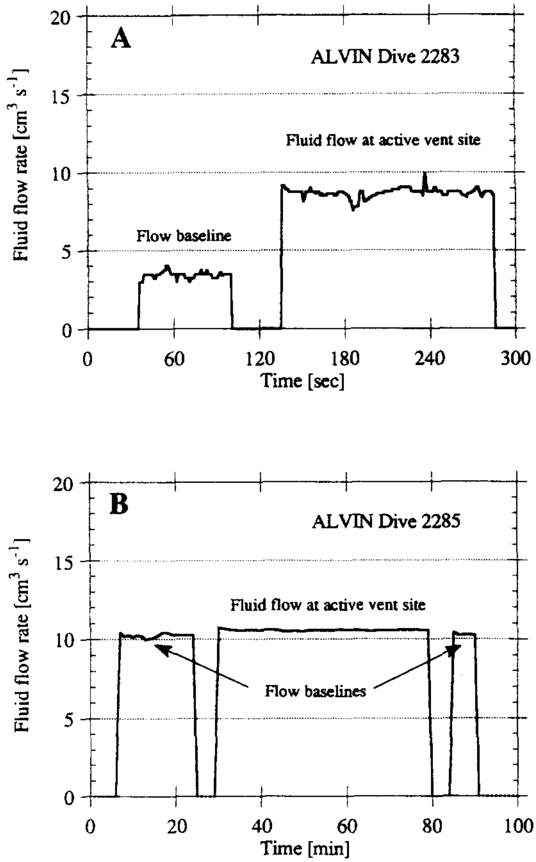

Fig. 4. (A) Fluid flow at *Alvin* dive sites 2283 and 2285 (B) measured with the thermistor flowmeter inserted into the exhaust port of the OSU Barrel. A zero flow signal (*in situ* baseline) was recorded while the flowmeter remained in a bucket mounted on the transport basket of the submersible *Alvin*. Flow data were calculated according to equation (6) from the strip chart recorder readings after recovery from the magnetic tape.

mounted on the transport basket of the D.S.R.V. *Alvin*. After inserting the flowmeter into the exhaust port at the top of the barrel and establishing a stable flow signal of 30–35 μA (mean 33 μA) for about 10 min, the signal was recorded on tape. By using the linear regression between observed flowmeter signal (μA) and output on the strip chart recorder (in scale units of mm) described in equation (5) the difference between both signals (measurement—zero flow), approximating 62 scale units, amounted to an actual outflow velocity of 0.99 cm s^{-1} based on the equation of the calibration graph (4).

The continuous record of flow data at the seep site (*Alvin* 2285) taken onboard the submersible revealed a signal of 81 scale units (after decoding the flowmeter readings from the tape recorder), whereas a zero flow signal of 75 scale units was recorded. After converting these signals to velocity (1.65 and 0.65 cm s^{-1}, respectively, see Fig. 4A) by using equation (6), the difference between both measurements yields an actual outflow velocity of 1 cm s^{-1}, which agrees with the velocity obtained from the observed ampere

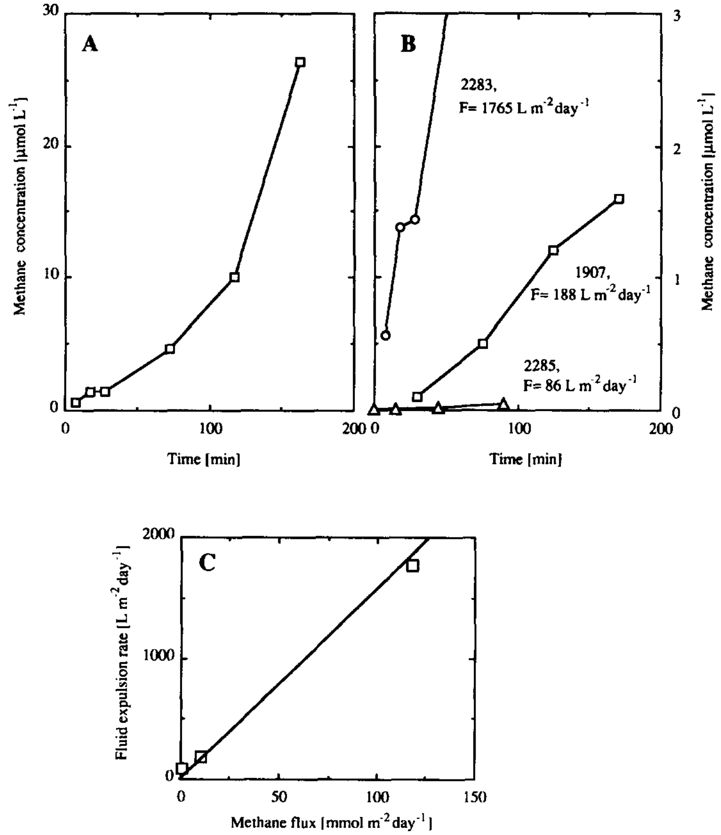

Fig. 5. (A) and (B) Increase in methane concentration with time for deployments at *Alvin* dive sites 2283, 2285 (this study) and 1907 (Carson *et al.*, 1990); the flow rates measured directly with flowmeters at each site are indicated by the letter "F". Note the different scales. (C) Relationship between mass fluxes of methane and fluid expulsion rates measured with the mechanical flowmeter at site 1907 (Carson *et al.*, 1990) and with the thermistor flowmeter at sites 2283 and 2285 (this study).

meter readings. Thus the actual fluid flow calculated according to equation (1) amounts to 5.31 $cm^3 s^{-1}$. This yields a flow of 459 l day^{-1} from the barrel, which has a bottom surface area of 0.26 m^2, and therefore a total fluid flow rate of 1765 l $m^{-2} day^{-1}$ (Table 1).

During this deployment an enormously vigorous methane flux was obtained from the sequential water sampler inside the barrel. Methane was stripped from the samples and measured by gas chromatography using an FID detector (Schmitt *et al.*, 1991); the sensitivity of the method ranges from 10 to 30 nl $CH_4\ l^{-1}$ (better than 0.001 μmol $CH_4\ l^{-1}$). The concentration of methane rose from 13 to 458 μmol l^{-1} over a period of 162 min; normally vent waters contain about 1 to 10 μmol $CH_4\ l^{-1}$. The increase in methane content inside the barrel was not linear but increased with increasing time of deployment (Fig. 5A). This could be due to initially incomplete mixing of the incoming vent water with the enclosed ambient bottom water or could be due to consumption of methane during the deployment. Hence we would underestimate the methane flow. These and other implications in deriving total mass fluxes from concentration measurement with the Benthic

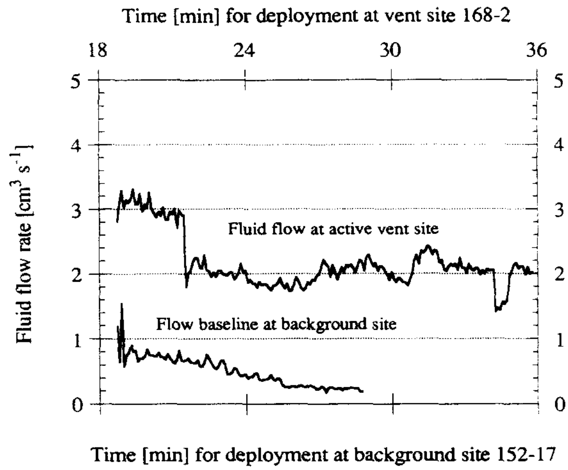

Fig. 6. Fluid flow recordings when VESP was deployed from the R.V. *Sonne* in the northern Peru basin (Sta. 152-17) to obtain a baseline under *in situ* conditions but without active venting, and the recordings at the Peru margin (Sta. 168-2) on an active seep site. The fluid expulsion rate at Sta. 168-2 was calculated using the increase of fluid flow over the background values (Table 1).

Barrel are discussed elsewhere (SUESS *et al.*, in preparation); it suffices here to report that the minimum CH_4-flux measured at *Alvin* dive site 2283 was 118 mmol m^{-2} day^{-1}.

During *Alvin* dive 2285, the barrel was deployed for 90 min over a sparsely populated *Solemya* clam field at 2424 m of depth. The continuous record of flow data over a period of 50 min at this site revealed a signal of 82.18 scale units, whereas zero flow amounted to 82 scale units. After converting these signals to velocity (1.98 and 1.93 cm s^{-1}, respectively, see Fig. 4B) by using equation (6), the difference between both measurements yields an actual outflow velocity of only 0.05 cm s^{-1}. This corresponds to an actual fluid flow rate of 86 l m^{-2} day^{-1} (Table 1). The concentration of methane rose from 0.015 to 0.051 μmol l^{-1} during the 90 min of the deployment (Fig. 5B).

TV-guided remote deployments

Several VESP-deployments were conducted in April 1992 during the R.V. *Sonne* cruise 78 to the continental margin off Peru (SUESS *et al.*, 1992). A previous survey with the French deep-sea submersible *Nautile* revealed active vent fields in two tectonic settings: in the accretionary prism at the base of the continental slope and along a fault-scarp created by a submarine landslide (BOURGOIS *et al.*, in press). A preliminary deployment of VESP in the northern Peru basin (07°04.6′S, 88°27.8′W, 4162 m water depth) was performed to obtain information about the background values for the chemical constituents (e.g. oxygen, methane, helium, trace metals) and the actual fluid flow in an area not influenced by subduction processes and active venting. Figure 6 shows the actual record obtained from the thermistor flowmeter during the background deployment in the northern Peru basin. During the first 2 min the flow measurements showed higher flow values, probably due to the generation of internal turbulences immediately after deployment of the barrel on the seafloor. The flow gradually declined to a constant value of 0.25 cm^3 s^{-1} (mean 0.44 cm^3 s^{-1}), which can be regarded as a baseline flow under *in situ* conditions

Table 1. *List of stations with venting rates obtained from* in situ *measurements, compared with indirect estimates using fluxes of methane and barium and temperature changes within the sediments*

Location	Position	Depth (m)	Approach	Flow rates ($l\ m^{-2}\ day^{-1}$)	Linear flow velocity ($m\ y^{-1}$)	References
Cascadia	44°40.44′N	2046	Mechanical flowmeter	188 ± 20	113	CARSON *et al.* (1990)
Alvin 1907	125°17.63′W		Methane flux	156 ± 10	95	CARSON *et al.* (1990)
			Porosity reduction	$\sim 1.8 \times 10^{-3}$		CARSON *et al.* (1990)
			Porosity reduction	$\sim 7 \times 10^{-4}$		HEMPEL and SUESS (in press)
			Heat flow	$\sim 4 \times 10^{-2}$	2.5×10^{-2}	DAVIS *et al.* (1990)
Cascadia	44°40.42′N	675	Thermistor flowmeter	1765 ± 20	1065	This study
Alvin 2283	125°07.49′W		Methane flux	1700* ± 50	1023	This study
Cascadia	45°56.19′N	2424	Thermistor flowmeter	86 ± 20	52	This study
Alvin 2285	125°20.82′W		Methane flux	50 ± 20	30	This study
Peru margin	9°35.26′S					
Sonne 168-2	80°07.70′W	3672	Thermistor flowmeter	441 ± 20	265	This study
Sonne 180-4	5°36.00′S	3309	Barium flux	970 ± 50	583	TORRES *et al.* (submitted)
	81°38.61′W					
Peru margin	5°36.32′S					
Nautile NP2-35	81°38.63′W	3540	Methane flux	200* ± 50	120	DIA *et al.* (submitted)
Nankai Trough			Heat flow		100	HENRY *et al.* (1992)
			Seismic velocity	$\sim 8 \times 10^{-4}$	6×10^{-4}	BEKINS and DREISS (1992)

Notes: the flow rates indicated by asterisks (*) were calculated assuming that the methane concentration in the feed water was the same as that for *Alvin* dive site 1907. The flow rates based on porosity reduction (steady-state dewatering) are averages over the entire prism, and therefore should not be directly compared with the flow rates obtained at an individual venting site. The linear flow velocity was estimated using a constant porosity of 60%.

(temperature, pressure, salinity and viscosity), but without active venting. The sediment surface at this station was very soft, and thus a very good seal between the barrel and surface sediments was achieved (Plate 2C). Therefore, an outflow due to an insufficient sealing at the sediment surface can be excluded. Figure 6 shows also the results of a successful deployment over an active seep site at the Peru margin (3672 m water depth, Table 1), where a mean fluid flow rate of 1.99 $cm^3 s^{-1}$ was directly measured. The sediment surface at this site was rough and covered with mudstone ledges and clam shells and only a thin layer of sediment (Plate 2D), allowing little penetration of the barrel. The actual fluid flow estimated from these values amounts to 441 l m^{-2} day^{-1} (Table 1). The accompanying methane flux at this site was insignificant, although a regionally elevated CH_4-anomaly pattern was observed. This was surprising since at all other vent sites previously investigated, CH_4 always was the most obvious indicator for venting. However, an unusual discovery of liquid higher hydrocarbons, emanating from this seep site, could explain the minor role which methane played here (SUESS *et al.*, 1992).

DISCUSSION

The discovery of active discharge of fluids and gases in subduction zones, collision zones of oceanic and continental plates and from areas which are not obviously effected by plate tectonic forces, has opened up new aspects in existing views of the marine cycle of matter. The magnitude of material transport from these geological settings are still largely unknown and are predominantly unquantified. It is certain, however, that the chemically mobile compounds of carbon, methane and carbon dioxide play a prominent role in the dewatering of collision zones just as they do in oceanic spreading zones. In these environments several attempts have been made to determine water and dissolved material flux rates by the use of submersibles (CARSON *et al.*, 1990; SAYLES and DICKINSON, 1991). These attempts consisted essentially of placing a sampling chamber "a benthic barrel" over active vent sites.

In this paper we have presented the results of the direct measurement of fluid flow from a submersible with a thermistor flowmeter from two deployments at the Cascadia subduction zone during *Alvin* dives 2283 and 2285 in 1990. During an earlier deployment in 1988 (dive 1907), *Alvin* visited an active seep site located at 2046 m of depth atop the back-thrust of the first accretionary ridge; a tectonic setting described by KULM *et al.* (1986) and MOORE *et al.* (1991). At this deployment the OSU Barrel was equipped with the mechanical flowmeter and with six Niskin™ bottles as reported by CARSON *et al.* (1990). Water samples were collected sequentially inside the barrel while it was placed over the seep site for 207 min. After completion of the sampling cycle, the flowmeter was inserted and a constant reading recorded for at least 15 min. The corrected water flow reported by CARSON *et al.* (1990) was 188 l m^{-2} day^{-1}. The flux rate of methane, assuming no consumption during deployment, was 10.3 mmol m^{-2} day^{-1}. Using this flux rate and the methane concentration in the sediment pore fluids which feed the seep, an estimated flow rate of 156 l m^{-2} day^{-1} can be obtained (CARSON *et al.*, 1990). The "true" water flow rate at *Alvin* dive site 1907, therefore, lies between 156 and 188 l m^{-2} day^{-1}. The two estimates are independent of each other, yet both were obtained by a single deployment of the OSU Barrel.

We can now compare the results reported by CARSON *et al.* (1990) to the new measurements obtained with the thermistor flowmeter (Table 1). This improvement allows for the continuous recording over extended periods of flow, more accurate and sensitive measurements, and the avoidance of back-pressure effects inherent in the mechanical flowmeter which required correction with a large uncertainty (CARSON *et al.*, 1990). The deployment during *Alvin* dive 2283 was at 675 m of water depth on the second accretionary ridge along a fault off-setting the seafloor. This fault intersects a subsurface gas hydrate layer and thereby gives rise to vigorous venting of methane (CARSON and HOLMES, 1991; MOORE, 1991: MOORE *et al.*, 1991). This site has been successfully drilled by the JOIDES Resolution (Leg 146) to determine the deeper plumbing system.

Alvin dive site 2285, in contrast, is characterized by low methane fluxes; however, venting at this site was inferred by the presence of numerous individuals of the bivalve *Solemya* sp. This site was located at the deformation front on the abyssal plain, under 2424 m of water, and is thought to emit deeply sourced fluids from the oceanic basement (MOORE *et al.*, 1991). Site 2285 also yielded a short sediment core from which methane was extracted by the blender method described by FABER and STAHL (1983). The total methane concentration measured in two samples from this core yielded values of $6.25 \pm 0.06\,\mu$mol kg^{-1} of wet sediment. This methane content includes a large fraction of adsorbed methane (approximately 60%), which is not capable of freely moving with the vent water and has to be subtracted. Therefore, we can estimate the free methane in the feed water to be 8 ± 3 μmol CH_4 l^{-1}, using a value for the wet bulk density of 1.4 g ml^{-1} and assuming a porosity of 80%. Using the methane concentration in the feed water, in conjunction with the methane flux measured in the barrel samples (Fig. 5), we obtained an independent fluid flow rate of 50 ± 20 l m^{-2} day^{-1} at this site (Table 1).

No sediment core, however, could be obtained for the characterization of the feed water at dive site 2283, because little sediment is being deposited at this site. Assuming that the water and the methane fluxes are both accurate at these sites, the feed water at dive site 2283 should contain approximately 66 μmol CH_4 l^{-1}. This is identical to the value previously obtained from the pore water at dive site 1907; an assumption that we consider valid given the proximity of the two sites and the similarity in subsurface plumbing and fluid source. Hence, we think that the same type of fluid is vented at the first and second ridge at the Cascadia margin off Oregon, albeit at very different rates (Table 1). This is also demonstrated by the very good agreement between the flow rates measured with the thermistor flowmeter and the methane fluxes for all the three sites surveyed (Fig. 5C).

The consistency between water flow and methane expulsion among the Cascadia dive sites over almost two orders of magnitude may be reasonably realistic for different tectonic settings in accretionary margins and show the applicability of using short-term experiments from submersibles to obtain such data. Furthermore, the mass fluxes of methane reported here for the first time clearly illustrate the enormous variability in the rates of fluid expulsion even within the same accretionary prism.

As described above, the results from the Peru margin, using the TV-controlled frame for deployment of the barrel, provide yet another measurement of fluid flow from cold seeps in convergent margins. Table 1 summarizes the values obtained by *in situ* measurements of flow in three settings on the Cascadia margin and from one station on the Peru slope. These values are compared with estimates using dissolved flow rates at these sites, as well as other indirect approaches used in the Nankai accretionary margin. These, to the best of our knowledge, are all the available data. Calculations using dewatering estimates based on porosity reduction (CARSON *et al.*, 1990; DAVIS *et al.*, 1990; BEKINS and DREISS, 1992; HEMPEL and SUESS, in press) are orders of magnitude lower than expected from mass flux calculations, subbottom temperature and direct flow measurements (LE PICHON *et al.*, 1992; CARSON *et al.*, 1990). This implies that only a small area of the total convergent margin is actually venting and that there also must be recharge zones associated with venting at these sites. Furthermore, steady-state compactive dewatering models, integrating over a long period of time, clearly underestimate mass transport rates from accretionary margins by not taking into account recirculation pathways.

The *in situ* flow measurements and indirect estimates from methane fluxes in the Cascadia margin yield surprisingly similar rates at each site; lending credibility to the approach of using an *in situ* instrumentation of the sea floor as developed by us. Vertical subbottom temperature profiles made inside a clam colony on Nankai in 1985 were used to infer an upward Darcy flow of about 100 m y^{-1} (HENRY *et al.*, 1989). Further measurements during the Kaiko–Nankai submersible survey confirmed the estimates of Darcy flow velocities in the range of 70–150 m y^{-1}. These results correspond approximately to the values obtained at *Alvin* dive site 1907 in the Cascadia margin. For comparison all *in situ* flow measurements are converted to vertical flow velocities either assuming realistic porosities or using actual geotechnical data obtained from sediment cores at *Alvin* dive sites 2285 and 1907.

In situ measurements and indirect estimates of fluid flow on the Peru slope give values of 441 and 200 l m^{-2} day^{-1}. All these data show the variability of venting rates among convergent margins, and even within the same tectonic setting, and clearly stress the need for a wider database in order to extrapolate these results in the global context of material cycling. Direct measurements and indirect estimates using dissolved mass balances and subbottom temperatures are all valid and independent means to evaluate fluid flow mass transport rates. The ability for deployment of instruments capable of performing these measurements from conventional research vessels using the TV-deployment system described here, will allow easier access to seep sites and a more widespread collection of the data needed to evaluate geochemical processes resulting from venting at cold seeps on a global basis.

Acknowledgements—We wish to thank the pilots of the D.S.R.V. *Alvin* and crews of the R.V.s *Atlantis* II and *Sonne* for logistical support, skillful deployment and recovery of the different experimental instruments. We greatly appreciate the technical support of Peter Kalk (Oregon State University), Arnim Flügge (Geology Dept., University of Kiel) and Peter Schymatzek (Technical support staff, R.V. *Sonne*). Financial support for this project was provided by the Bundesministerium für Forschung und Technologie (Projects 03R607 6 and 03R418 9) and by the National Science Foundation (Project OCE 8609789). This is publication no. 157 of the Sonderforschungsbereich 313, supported by the Deutsche Forschungsgemeinschaft.

REFERENCES

BARNETT P. R. O., J. WATSON and D. CONELLY (1984) A multiple corer for taking virtually undisturbed samples from shelf, bathyal and abyssal sediments. *Oceanologica Acta*, **7**, 399–408.

BEKINS B. A. and S. J. DREISS (1992) A simplified analysis of parameters controlling dewatering in accretionary prisms. *Earth and Planetary Science Letters*, **109**, 257–287.

BOULÈGUE J., J. T. LIYAMA, J.-L. CHARLOU and J. JEDWAB (1987) Nankai Trough, Japan Trench and Kuril Trench: geochemistry of fluids sampled by the submersible *Nautile*. *Earth and Planetary Science Letters*, **83**, 363–375.

BOURGOIS J., Y. LAGABRIELLE, P. DEWEVER, E. SUESS and THE NAUTIPERC CRUISE SHIPBOARD SCIENTISTS (in press) Tectonic history of a non accreting active margin during the past 400 ka. Results of a submersible survey of the Peru Trench at 5–6°. *Geology*.

CARSON B. and M. L. HOLMES (1991) Fluid expulsion sites imaged on Cascadia margin. *News from the JOI/U.S. Science Support Program Associated with the Ocean Drilling Program*, **4**, 5–12.

CARSON B., E. SUESS and J. STRASSER (1990) Fluid flow and mass flux determinations at vent sites on the Cascadia Margin accretionary prism. *Journal of Geophysical Research*, **95**, 8891–8897.

DAVIS E. E., R. D. HYNDMAN and H. VILLINGER (1990) Rates of fluid expulsion across the northern Cascadia accretionary prism: constraits from new heat flow and multichannel seismic reflection data. *Journal of Geophysical Research*, **95**, 8869–8888.

DIA A. N., L. AQUILINA, E. SUESS, M. TORRES, J. BOULÈGUE and J. BOURGOIS (submitted) Continent derived fluids from the convergent margin off Peru. Deep sea dives of the Nautiperc cruise, Part 2. *Geology*.

FABER E. and W. STAHL (1983) Analytical procedure and results of an isotope geochemical surface survey in an area of the British North Sea. In: *Petroleum, geochemistry and exploration of Europe*, J. BROOKS, editor, Blackwell, London, pp. 51–63.

HEMPEL P. and E. SUESS (in press) Dewatering of sediments along the Cascadia margin: evidence from geotechnical properties. Proceedings of the Ocean Drilling Program, Initial Reports ODP Leg 146.

HENRY P., S. J. LALLEMANT, X. LE PICHON and S. E. LALLEMAND (1989) Fluid venting along Japanese trenches, tectonic context and thermal modelling. *Tectonophysics*, **160**, 277–292.

HENRY P., J.-P. FOUCHER, X. LE PICHON, M. SIBUET, K. KOBAYASHI, P. TARITS, N. CHAMOT-ROOKE, T. FURUTA and P. SCHULTHEISS (1992) Interpretation of temperature measurements from the Kaiko–Nankai cruise: modelling of fluid flow in clam colonies. *Earth and Planetary Science Letters*, **109**, 355–371.

KULM L. D., E. SUESS, J. C. MOORE, B. CARSON, B. T. LEWIS, S. D. RITGER, D. KADKO, T. M. THORNBURG, R. EMBLEY, W. RUGH, G. MASSOTH, M. LANGSETH and G. COCHRANE (1986) Oregon margin subduction zone: venting, fauna and carbonates. *Science*, **231**, 561–566.

LABARBERA M. and S. VOGEL (1976) An inexpensive thermistor flowmeter for aquatic biology. *Limnology and Oceanography*, **21**, 750–756.

LEPICHON X., K. KOBAYASHI and KAIKO-NANKAI SCIENTIFIC CREW (1992) Fluid venting activity within the eastern Nankai Trough accretionary wedge: a summary of the 1989 Kaiko–Nankai results. *Earth and Planetary Science Letters*, **109**, 303–318.

MOORE J. C. (1991) Geophysicists meet bioherm: seepy story surfaces. *News from the JOI/U.S. Science Support Program Associated with the Ocean Drilling Program*, **4**, 1–3.

MOORE J. C., A. MASCLE and LEG 110 SHIPBOARD SCIENTISTS (1987) Expulsion of fluids from depth along a subduction-zone decollement horizon. *Nature*, **326**, 785–788.

MOORE J. C., K. M. BROWN, F. HORATH, G. COCHRANE, M. MACKAY and G. MOORE (1991) Plumbing accretionary prisms: effects of permeability variations. *Philosophical Transactions of the Royal Society of London A*, **335**, 275–288.

SAYLES F. L. and W. H. DICKINSON (1991) The seep meter: a benthic chamber for the sampling of low velocity hydrothermal vents. *Deep-Sea Research*, **38**, 129–141.

SCHMITT M., E. FABER, R. BOTZ and P. STOFFERS (1991) Extraction of methane from seawater using ultrasonic vacuum degassing. *Analytical Chemistry*, **63**, 529–532.

SUESS E., B. CARSON, S. D. RITGER, J. C. MOORE, L. D. KULM and G. R. COCHRANE (1985) Biological communities at vent sites along the subduction zone off Oregon. In: *The hydrothermal vents of the Eastern Pacific: an overview*, M. C. JONES, editor, *Bulletin of the Biological Society of Washington*, **6**, 475–484.

SUESS E. and THE SO 78 CRUISE SHIPBOARD SCIENTISTS (1992) FS Sonne: Fahrtbericht SO 78 Peruvent. Balboa, Panama–Balboa. Panama 28.2.1992–16.4.1992. *GEOMAR Report*, **14**, 120 pp.

TORRES M., A. DIA, J. BOULÈGUE, L. AQUILINA and E. SUESS (submitted) Barite deposits from the Peru subduction zone. *Earth and Planetary Science Letters*.

VOGEL S. (1981) *Life in moving fluids. The physical biology of flow*. Willard Grant Press, Boston, 352 pp.